forests

MDPI

Article

Synergistic Effects of Heating Platens' Temperature and Compression Ratio on the Periodic Hot-Press Drying of Chinese Fir Lumber

Xiang Weng [1], Xingying Zhang [2], Chengjian Huang [3,*], Shipeng Wang [2] and Junfeng Hou [2,*]

[1] College of Mathematics and Computer Science, Zhejiang A&F University, Hangzhou 311300, China; woodweng@zafu.edu.cn
[2] College of Chemistry and Materials Engineering, Zhejiang A&F University, Hangzhou 311300, China; zxy12138@stu.zafu.edu.cn (X.Z.); gu3241984489@stu.zafu.edu.cn (S.W.)
[3] China National Bamboo Research Center, Hangzhou 310012, China
* Correspondence: hcj5236@yeah.net (C.H.); houjunfeng@zafu.edu.cn (J.H.)

Abstract: The effects of periodic hot-press drying on drying behavior and mechanical damage to Chinese fir lumber were investigated by taking the heating platens' temperature (T_P) and compression ratio (R_c) as experimental factors. The temperature and pressure inside lumber were analyzed during drying process. The results were as follows. The drying rate of lumber was significantly increased with increasing T_P and R_c. Scanning electron microscope (SEM) micrographs showed that bordered pit membranes, cross-field pits, middle lamella between adjacent cells, and tracheid walls were damaged after drying, and the damage became more severe with higher T_P and R_c. Detachments between ray parenchyma cells and tracheids were observed at 170 °C. Nitrogen-adsorption measurement results demonstrated that more cell wall pores in the 2.5~6.2 nm pore diameter range were generated at higher T_P, resulting in an enlarged specific surface area and pore volume of cell walls. These structural changes contributed to accelerating moisture migration and decreasing the drying time. Furthermore, fluctuating pressure inside lumber was the main driving force leading to moisture migration and cell tissue damage in lumber during drying. The influence of T_P on internal temperature (T_M) and pressure (P_M) was greater than R_c. With the increase in T_P from 130 to 170 °C at the R_c of 10%, the maximum T_M and P_M were increased by 30.90% and 39.84%, respectively. However, T_P should not be too high to prevent the formation of macro-cracks caused by high pressure, which may significantly affect wood's mechanical properties. These results provide theoretical support for periodic hot-press drying processes' improvement and high-value utilization of Chinese fir.

Keywords: periodic hot-press drying; Chinese fir lumber; mechanical damage; temperature; pressure

Citation: Weng, X.; Zhang, X.; Huang, C.; Wang, S.; Hou, J. Synergistic Effects of Heating Platens' Temperature and Compression Ratio on the Periodic Hot-Press Drying of Chinese Fir Lumber. *Forests* **2024**, *15*, 203. https://doi.org/10.3390/f15010203

Academic Editor: Sofia Knapic

Received: 10 December 2023
Revised: 7 January 2024
Accepted: 11 January 2024
Published: 19 January 2024

1. Introduction

Chinese fir (*Cunninghamia lanceolata* (Lamb.) Hook.) is a major commercial plantation, species with the largest planting area and accumulation in South China [1]. Nevertheless, Chinese fir is known as a refractory species and needs long periods of drying, resulting in high energy consumption and more drying defects [2]. In addition, its rapid growth rate and a large proportion of juvenile wood cause a low wood density and soft material properties, which adversely affect the quality of wood products [3]. These problems seriously restrict the high-value utilization of Chinese fir, and techniques to accelerate the drying rate and to improve wood properties are obviously indispensable.

Hot-press drying is a useful and proven technique for reducing the drying time and strengthening the wood surface [4–6]. Wood lumber is subjected to compression forces from two heated platens during the drying process, with the aim of increasing the drying rate and reducing the warp [7,8]. Compared with conventional drying, hot-press drying can

shorten the drying time from several days to 1~2 h due to good heat transfer from the platen to the wood [9]. Furthermore, the mechanical pressure of heating plates keeps the lumber flat during drying, thereby reducing the amount of drying degradation caused by wood warping and deformation [10,11]. The density and dimensional stability of lumber can also be improved due to the effect of thermal and compression treatment [9,11]. Therefore, research on hot-press drying of Chinese fir is of theoretical significance for the efficient and high-value utilization of this resource.

Heat and mass transfer play a key role in the drying process of wood [12]. In the process of hot-press drying, the heat of heating platens transfers from the abaxial and adaxial surfaces to the center along the thickness orientation of dried lumber. The heat transfer medium is composed of free water, bound water, steam, and substance inside the wood. Moisture migration is mainly driven by the pressure difference between the dried lumber and the atmospheric environment, which is caused by the rapid vaporization of water inside the wood at high temperatures, resulting in an increase in steam pressure [13–15]. The increasing pressure also causes damage to each cell tissue of wood to various degrees and open moisture passages, which leads to increased migration efficiency of moisture [16,17]. However, if the steam pressure is too high, the damage to cell tissues will become larger, resulting in internal cracking and other drying defects, thereby reducing the drying quality of wood [18,19]. It can be seen that the study of temperature and pressure in lumber is very important to reveal the hot-press drying mechanisms and to optimize the parameters of the drying process. Nevertheless, most previous correlational studies focused on the internal temperature of lumber [20,21], and the steam pressure was considered in a limited way and was always theoretically calculated according to the ideal gas equation. The experimental investigation of steam pressure inside lumber was seldom reported. In addition, the extent of damage to wood cell tissues is closely related to the drying rate and quality. Although previous studies have investigated the microstructure of hot-press dried wood [22–25], little effort has been found focusing on the systematic investigations of Chinese fir wood.

In this study, Chinese fir lumber was periodically hot-press dried at different heating platens' temperatures (T_P) and compression ratios (R_c). The effects of periodic hot-press drying on drying rate, microstructure, and cell wall pore structure of Chinese fir lumber were systemically studied. The internal temperature and steam pressure variations of lumber during drying process were analyzed to reveal the influence mechanism of T_P and R_c on moisture migration and mechanical damage to dried lumber. The purpose of this study was to provide a theoretical basis for precise control of the hot-press drying process for wood and realize the value-added utilization of fast-growing wood.

2. Materials and Methods

2.1. Materials

Chinese fir logs were collected from Quzhou City in Zhejiang Province in China. The corresponding air-dried density of this wood species was 0.358 ± 0.010 g·cm^{-3}. Lumber with dimensions of 400 (Longitudinal) × 100 (Tangential) × 30 (Radial) mm^3 was sawed from these logs. The initial MC of lumber was adjusted to 50% to 60% before periodic hot-press drying.

2.2. Periodic Hot-Press Drying of Chinese Fir Lumber

Periodic hot-press drying of Chinese fir lumber was performed with a single-opening hot press (XLB-D500 × 500, Huzhou Dongfang Machinery Co., Ltd., Huzhou, China), and the dimension parameters of the heating platen were 500 mm (Length) × 500 mm (Width). The drying schedule is shown in Table 1.

Table 1. Drying Schedule of Chinese fir lumber during periodic hot-press drying.

Sample No.	Heating Platens' Temperature (°C)	Preset Compression Ratio (%)	Preset Final Thickness (mm)
A	130	10	27
B	170	10	27
C	130	30	21
D	170	30	21

Before drying, two platens were preheated to 130 and 170 °C. The specimen was then placed in a hot press with a pressure of 2 MPa applied in the radial direction, with the aim to compress the lumber from the initial to a target thickness. The preset compression ratios (R_c, the ratio of the reduced thickness to the initial thickness) of the lumber were 10% and 30%. A thickness gauge was applied to maintain the required thickness of the lumber. The heated platens remained closed and were opened intermittently, so a number of closing–opening cycles (also known as breathing cycles) were formed during the drying process. The heating platens' closing duration was 10 min, and their opening time was 2 min in a breathing cycle. A final MC of dried lumber was determined according to China National Standard (Drying quality of sawn timber, GB/T 6491-2012) [26].

2.3. Internal Temperature (T_M) and Pressure (P_M) of Lumber during Drying

T_M and P_M of lumber was monitored with a press monitoring system (PressMAN™ Lite, Alberta Research Council, Edmonton, AB, Canada) embedded in the central layer of the lumber, as illustrated in Figure 1 [15]. A hole with a 1.82 mm diameter was prepared in the core layer of dried lumber, and its depth was 50 mm in the tangential orientation. The real-time measurement of T_M and P_M were conducted using PC with a time interval of 1 s. The monitoring ranges of the pressure transmitter and temperature are 0~500 KPa and 0~500 °C, respectively. Both ends of the tested specimens were sealed with high-temperature-resistant epoxy resin to ensure that moisture only transferred along the radial orientation of lumber during drying. Two tested specimens were prepared during periodic hot-press drying. One of them was used to determine MC of lumber, and the other was used to monitor T_M and P_M inside lumber at the same time. Three replications corresponding to each group were measured for MC, T_M, and P_M.

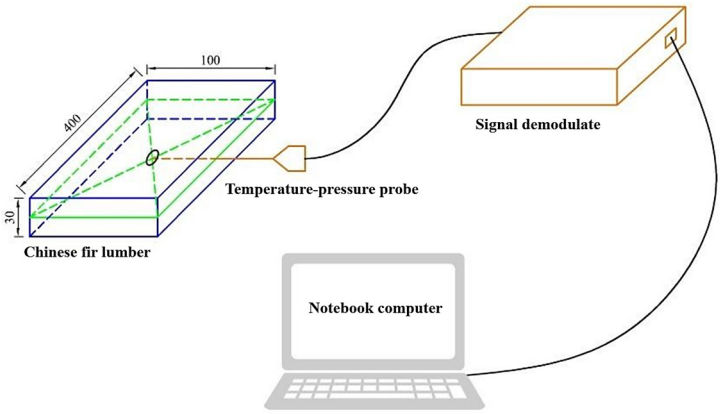

Figure 1. Connection and test method for the online monitoring system of temperature and pressure.

2.4. Microstructure and Pore Structure Analysis

In order to investigate the generation of mechanical damage to cell tissues after periodic hot-press drying, microstructural changes and the cell wall pore structure were characterized using a scanning electron microscope (TM-3030, Hitachi, Tokyo, Japan) and a fully automated specific surface area and pore size profiler (NOVA 4200e, Quantachrome,

Boynton Beach, FL, USA), respectively. Slices 70 μm in thickness with standard radial and tangential surface of wood specimens were prepared for microstructure observation. Pits and ray parenchyma cells were selected for primary analysis. The nitrogen adsorption method was used for pore structure analysis, and the specific surface area, pore volume, and pore size distribution of dried lumber were investigated.

3. Results

3.1. Drying Curves

Figure 2 presents the drying curves and average drying rate of Chinese fir lumber. The initial MC values of samples A, B, C, and D were all between 54.3% and 57.1%, and the final MC values were 7.2%, 6.8%, 7.4%, and 4.0%, respectively, which met the first drying grade requirements in accordance with China National Standard. The results also indicate that drying time was significantly reduced with increasing T_P and R_c. In comparison with Sample A, the drying time of Sample B was decreased by 50.00%, and that of Sample D was decreased by 38.46% compared to Sample C. Compared with Sample A and B at 10% R_c condition, the decrement of drying time for Sample C and Sample D at 30% R_c was 40.91% and 27.27%, respectively.

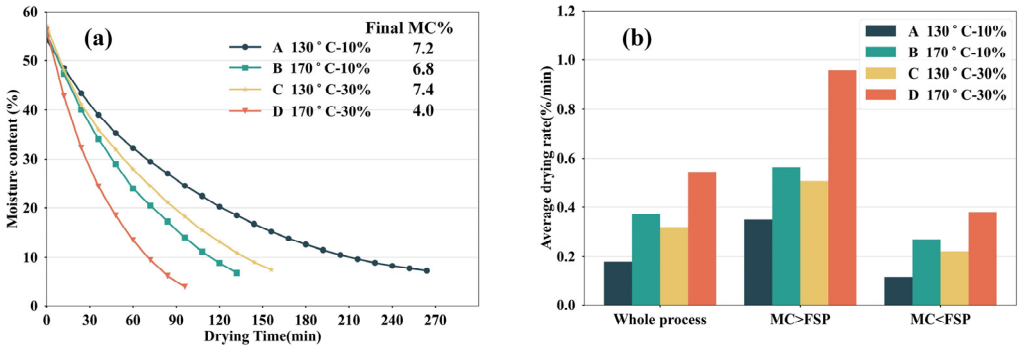

Figure 2. Drying curves (**a**) and average drying rate (**b**) of dried lumber.

The drying rate of wood samples is shown in Figure 2b. With increasing T_P, the average drying rate (whole process) of Sample B was increased by 107.87% in comparison with Sample A, and that of Sample D was increased by 70.53% in comparison with Sample C. Compared with Sample A and B at 10% R_c, the increments in drying rate (whole process) for Sample C and Sample D at 30% R_c were 79.21% and 47.03%, respectively. Additionally, an obvious increase in the drying rate was generated in the early (MC > FSP) and later stages (MC < FSP). This phenomenon indicated that the moisture migration (both free water and bound water) during the drying process was accelerated with increasing T_P and R_c. This finding was in accordance with the study by Zhou et al. [27]. The reason for such trends may be the greater amount of heat transferred from the heating platens to dried lumber per unit time at the greater T_P, indicating the higher maximum temperature and steam pressure obtained inside lumber, thereby increasing the pressure gradient between the core layer and the atmospheric environment and accelerating moisture migration. As the R_c increased, the heat-transfer path was shortened due to the decreased thickness of the lumber, which facilitated the acceleration of the transfer efficiency of heat. Thus, a more complete vaporization of water inside lumber was expected, resulting in a higher steam pressure and improved water removal from wood. Additionally, free water was efficiently removed from cell lumens under the action of mechanical compression pressure when the platens were closed. The greater R_c can also result in a larger volume of free water being removed from wood in each breathing cycle, thereby increasing the efficiency of free water removal.

3.2. Microstructural Changes in Dried Wood

In wood, the bordered pit is a crucial element in the circulation of axial intercellular fluid flow, which exhibits a significant effect on the permeability and drying properties of wood [28–30]. The pits in the heartwood of Chinese fir are usually covered by amorphous materials, and most of the pit membranes are encrusted, which severely hinder the migration of moisture [31]. Figure 3 shows the bordered pits of Chinese fir after hot-press drying. Some of the micro-fibrils in bordered pit membrane were fractured and formed cracks under a 130 °C/10% R_c condition (Figure 3b). With the increase in R_c from 10% to 30% at 130 °C, the cracks were enlarged, while the torus basically remained intact (Figure 3c). In the case of dried lumber in the 170 °C/10% R_c condition, all of the micro-fibrils were fractured and the torus became separated from the bordered pit membrane as well (Figure 3d). The results showed varying degrees of damage to the bordered pits, which became increasingly severe with higher T_P and R_c. This damage could potentially rupture aspirated pits and enhance wood permeability [32]. During hot-press drying, water inside the lumber vaporized rapidly, and a large amount of steam was generated. Damage in some weak tissues (i.e., pit membranes and ray cells) of anatomical structures was observed to be generated with the increase in steam pressure [33]. With increasing T_P and R_c, the heat transfer efficiency improved due to the greater temperature gradient between the heating platens and dried lumber, as well as the shorter heat transfer path. Thus, the water in wood vaporized more intensely, resulting in a higher level of internal pressure and a greater degree of damage to the pit membrane.

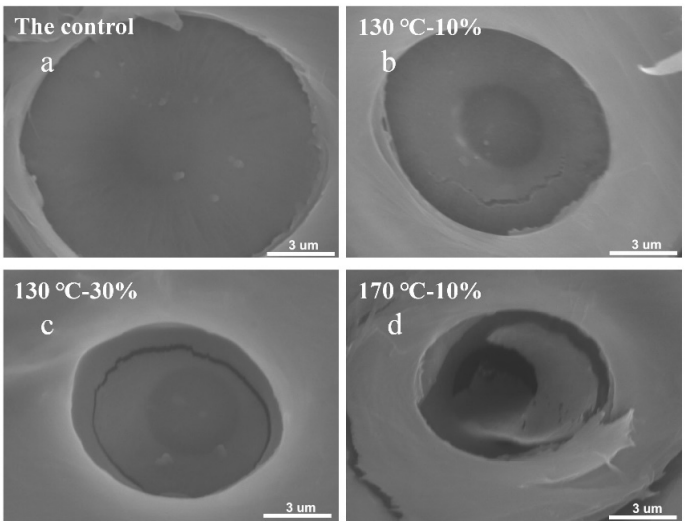

Figure 3. SEM micrographs of bordered pits inside lumber after drying under different conditions: (**a**) Control, (**b**) 130 °C-10%, (**c**) 130 °C-30%, (**d**) 170 °C-10%.

Cross-field pits serve as channels for the transfer of water and nutrients between the longitudinal and radial cells of wood. Figure 4 presents the cross-field pit region in Chinese fir after drying. In the control group, some extracts were observed to be located in the longitudinal tracheid cavities adjacent to ray parenchyma cells (Figure 4a). However, the amount of extract inside dried lumber was significantly reduced (Figure 4b–d). In the 130 °C/10% R_c condition, tiny cracks appeared at the ends of cross-filed pits, and the middle lamella between the tangential walls of tracheids was damaged (Figure 4b). The cracks were further expanded, propagating to the cell walls of tracheids with the increase in R_c from 10% to 30% (Figure 4c). In addition, the damage to the cross-filed pits became more severe, and the stratification phenomenon occurred in the ray parenchyma cells in the 170 °C/10% R_c condition (Figure 4d). Similar phenomena have been observed in previous studies involving steam-explosion-treated wood [28,34]. According to Muzamal's research,

high steam pressure can lead to stress concentration at the ends of cross-field pits, making them more vulnerable to damage [35].

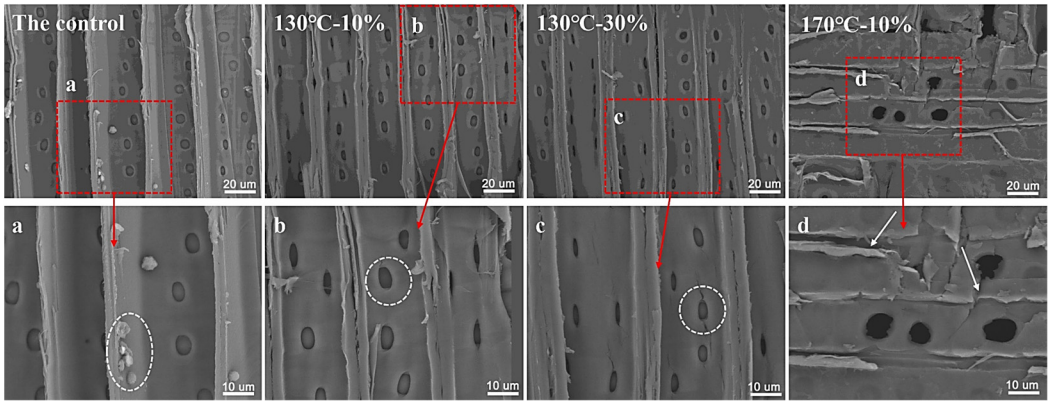

Figure 4. SEM micrographs of cross-field pits inside lumber after drying under different conditions: (**a**) Control, (**b**) 130 °C-10%, (**c**) 130 °C-30%, (**d**) 170 °C-10%.

SEM micrographs of the tangential sections of Chinese fir after drying are presented in Figure 5. A uniserial wood ray that consisted of ray parenchyma was observed, and the amount of extract inside the cell cavity of ray parenchyma was obviously reduced after hot-press drying. The reason was that free water and steam were transferred along the cell cavity of radial ray parenchyma under the action of steam pressure gradient, resulting in the fluxion and redistribution of extract [36]. It was also noted that obvious deformation was generated to the cell wall of the ray parenchyma with the increase in R_c from 10% to 30% at 130 °C (Figure 5c). This is due to the radial compression of the wood during the drying process, and the increase in R_c led to the increasing deformation of the ray parenchyma cells. Moreover, cracks in the middle lamella between ray parenchyma cells and longitudinal tracheids appeared at 170 °C (Figure 5d). The reason was that higher temperature and pressure inside the wood were generated with increasing T_P, and the middle lamella cracked due to the high pressure, resulting in the ray parenchyma cells and adjacent longitudinal tracheids being separated.

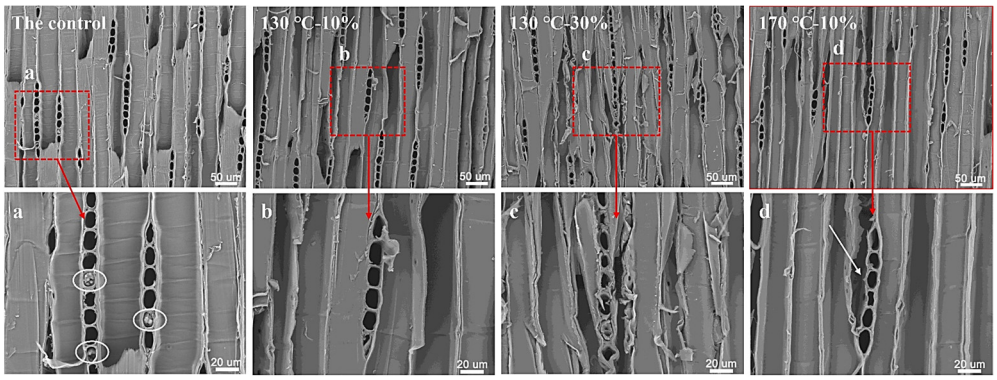

Figure 5. SEM micrographs of tangential section of lumber after drying under different conditions: (**a**) Control, (**b**) 130 °C-10%, (**c**) 130 °C-30%, (**d**) 170 °C-10%.

These microstructural changes may form new pathways for fluid flow and accelerate the migration of moisture between cells, which contribute to the increased permeability of Chinese fir wood and reduced drying time. The extent of damage to the wood microstructure was increased with increasing T_P and R_c, and T_P shows a greater effect on microstructure than R_c. Furthermore, T_P should not be too high to prevent the formation of macro-cracks caused by high pressure, which may significantly affect the wood's mechanical properties.

3.3. Pore Structure Variation in the Cell Wall of Dried Wood

The pore structure parameters of the Chinese fir wood cell wall after drying are shown in Table 2. An obvious increase in the specific surface area and pore volume of cell wall (SA-CW and PV-CW) were formed after drying. In comparison with the control, the SA-CW values of lumber dried at 130 and 170 °C under the 10% R_c were increased by 22.72% and 81.77%, respectively. And the corresponding increments in PV-CW were 5.10% and 73.06%, respectively. In the case of dried wood under the 30% R_c condition, the SA-CW values of lumber dried at 130 and 170 °C were increased by 37.79% and 91.37%, respectively, in comparison with the control. And the corresponding increments in PV-CW were 16.05% and 79.21%, respectively. Similar trends were reported by Yin et al. [37] on Chinese fir with compression and steam treatment, a large number of 3.7 nm pores were created in the cell wall due to the synergistic effect of external mechanical pressure and high-temperature steam, and the pore structure variation became more obvious with higher compression ratio and temperature. As a result, SA-CW and PV-CW were increased accordingly. In contrast, the average pore size was decreased with increasing T_P and R_c, which may be due to the greater number of small pores being generated.

Table 2. Pore structure parameters of wood cell wall after drying.

Sample No.	Specific Surface Area (m^2/g)	Pore Volume (cc/g)	Average Pore Size (nm)
The control	0.823	3.059×10^{-3}	33.417
A (130 °C-10%)	1.010	3.215×10^{-3}	29.727
B (170 °C-10%)	1.496	5.294×10^{-3}	24.882
C (130 °C-30%)	1.134	3.550×10^{-3}	27.997
D (170 °C-30%)	1.575	5.482×10^{-3}	21.231

The relationship between cumulative pore volume and pore diameter of the wood cell wall after drying is presented in Figure 6. The results showed that periodic hot-press drying has a sizable influence on the pore structure within the diameter range of 2.5~6.2 nm for the pores in the wood. The pore volumes (pore diameter: 2.5~6.2 nm) of lumber dried at 130 and 170 °C at 10% R_c were increased by 80.9% and 192.0%, respectively, in comparison with the control. The corresponding increments under the 30% R_c were 113.0% and 196.0%. However, the increment in pore volume was 1.2% with the increase in R_c from 10% to 30% at 170 °C. This may be due to the adequate softening of the cell wall at this temperature, so the effect of mechanical compression on the pore structure of the cell wall was limited.

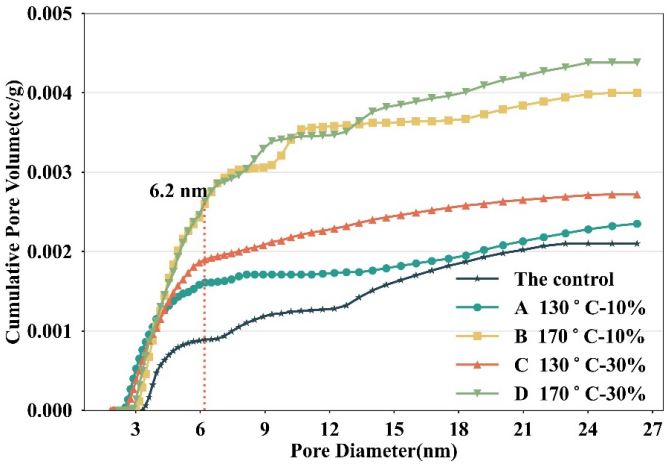

Figure 6. Relationship between cumulative pore volume and pore diameter of the wood's cell walls after drying.

Figure 7 shows the relationship between the pore volume and pore diameter of the wood's cell walls after drying, and the pore size distribution variation after drying can be analyzed. Compared with the control, more pores were generated in the pore diameter ranging from 2.5 nm to 6.2 nm at a T_P of 130 °C (Figure 7a,b), thereby increasing the pore volume within this pore diameter range. This may be attributed to the high steam pressure generated and mechanical compression during the drying process, which damaged cell walls and created new micro-voids. In addition, a greater number of pores were generated within the same diameter range at T_P of 170 °C (Figure 7c,d), and the number of pores with the other diameter range was also increased, which was possibly related to more severe damage to the pore structure of cell wall under this treatment condition.

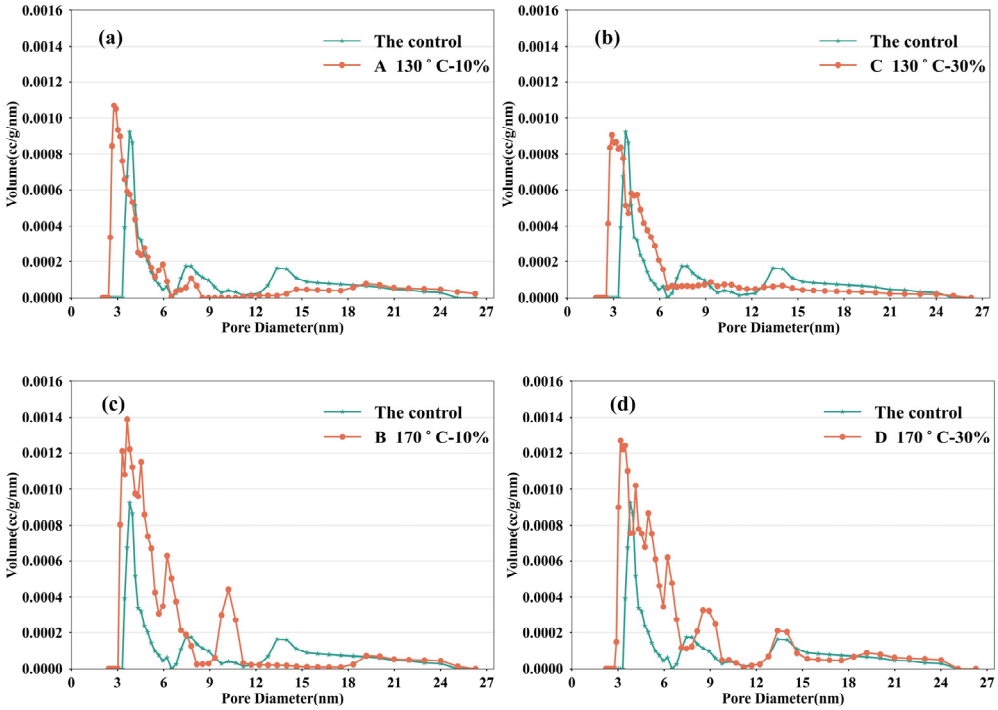

Figure 7. Relationship between pore volume and pore diameter of wood cell wall after drying under different conditions: (**a**) 130 °C-10%, (**b**) 130 °C-30%, (**c**) 170 °C-10%, (**d**) 170 °C-30%.

3.4. Temperature Behaviors

The internal temperature (T_M) behaviors of lumber during drying are shown in Figure 8. The T_M curves of lumber can be divided into three stages: rapid temperature increase, constant temperature, and slow temperature increase [17]. The T_M of lumber was increased rapidly from room temperature to a stable value in a short time during the first stage. This can be attributed the fact that heat was transferred from the heating platen to the core layer of lumber under the function of the great temperature gradient [38]. Furthermore, free water in the surface of lumber vaporized quickly at a high temperature, leading to a rapid rise in steam pressure [39]. Accordingly, a distinct pressure gradient between the evaporation front and the core layer of lumber was developed in the closing period of heating platens. Then, the free water and steam at the evaporation front were gradually moved to the core layer under the function of the pressure gradient, and a large amount of heat energy was transferred to the core layer, resulting in the rapid increase in T_M of lumber [14]. Fluctuations in the T_M of lumber occurred during the constant temperature stage. The reason was that the heat transferred in this stage was mainly used for the endothermic vaporization of free water. Therefore, T_M was maintained at the boiling point temperature of free water corresponding to internal steam pressure in accordance with the law of energy conservation and transformation [17]. Additionally, the superheated steam was generated with the further increase in drying time in the stage

of slow temperature increase. The T_M was moderately increased and close to the value of T_P. Heat was conducted through the diffusion of bond water and steam along the thickness orientation of lumber and heat conduction from lumber in this stage. Due to the decrease in the MC of lumber and the temperature gradient between the surface layer and the core layer, the heating rate of this stage is lower than that of the stage of rapid temperature increase.

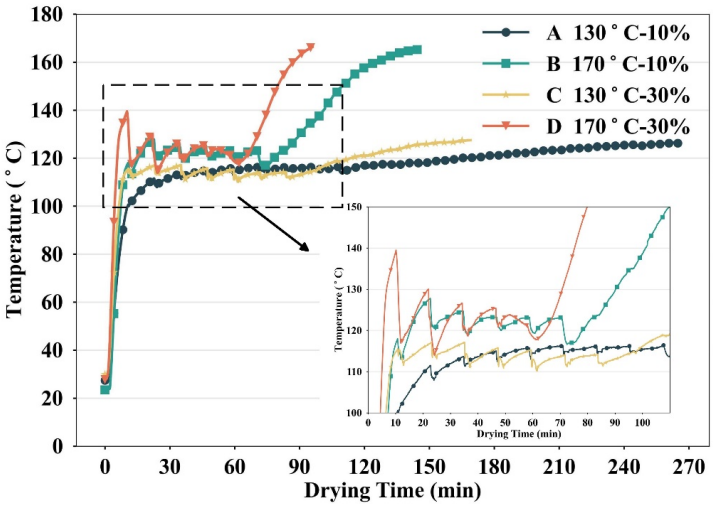

Figure 8. Curves of temperature in Chinese fir lumber as a function of time.

As illustrated in Figure 8, the heating rate of T_M increased with the increase in T_P, resulting in the greater maximum T_M in the constant temperature stage and the end of drying. With the increase in T_P from 130 to 170 °C at the R_c of 10%, the heating rate was increased from 3.69 °C/min to 8.82 °C/min in the rapid temperature-increasing stage. The corresponding stable temperature ranges were 107.9~116.5 °C and 113.4~127.8 °C, respectively. In the stage of a slow temperature increase, the heating rate was also increased from 0.08 °C/min to 0.67 °C/min. And the maximum T_M values inside dried lumber were 126.2 °C and 165.2 °C, respectively.

This phenomenon was because the temperature gradient along the thickness orientation of lumber increased with the increase in T_P, leading to an obvious increase in the amount of heat transferred from the heating platens to the dried lumber per unit time, thereby increasing the heating rate in the stag of rapid temperature increase. In addition, the vaporization of water inside lumber became more complete with a higher T_P, resulting in higher internal steam pressure and an increased boiling point temperature of free water corresponding to internal steam pressure. Thus, the stable temperature range was increased in the constant temperature stage. Furthermore, the T_M was moderately increased and close to T_P during the stage of a slow temperature increase. An obvious increase in the heating rate was generated with the increase in T_P in this stage, since a greater temperature gradient was generated between the surface layer and the central layer. Eventually, a higher maximum T_M could be achieved at higher T_P.

It was also found that the heating rate increased with increasing R_c. When R_c increased from 10% to 30% at the T_P of 130 °C, the heating rates were increased by 115.45% and 137.50%, respectively, in the stages with a rapid temperature increase and a slow temperature increase, respectively. The reason was that the higher R_c decreased the thickness of lumber and shortened the heat-transfer path, which contributed to improved transfer efficiency of heat originating from heating platens to the core layer of wood, thereby increasing the heating rate. However, the increase in maximum T_M is not obvious, indicating that the maximum T_M is mainly related to the T_P.

3.5. Pressure Behaviors

The curves of internal pressure (P_M) of lumber are presented in Figure 9. Obvious fluctuations in the P_M of lumber occurred with each breathing cycle of the drying process (Figure 9a). This indicates that P_M was increased and a peak value was obtained during the closing period of the heating platens. And P_M was decreased rapidly due to the steam discharge with the opening of heating platens. Figure 9b illustrates the curves of peak P_M with a breathing cycle. It was found that the peak values of P_M increased with the increase in the breathing cycle until the maximum P_M was obtained and then decreased with the further increase in the breathing cycle. The maximum P_M was increased by 39.84% with the increase in T_P from 130 to 170 °C at an R_c of 10%. In addition, the maximum P_M values in group A and B were obtained at breathing cycles of 5 and 2, respectively, suggesting that the higher T_P also increased the rate of peak P_M rise. The reason could be that a greater temperature gradient between the heating platens and lumber was developed, resulting from higher T_P, leading to an obvious increase in the heat-transfer efficiency. Therefore, the larger the amount of water vaporized inside the wood, the faster the rise in the peak P_M and the higher the maximum P_M obtained. In addition to this, the peak P_M of Group A was greater than that of Group B, with the breathing cycle extended to 7. The reason was that the MC of lumber sharply decreased with the breathing cycle being extended at 170 °C (Figure 2a). Thus, the amount of water vaporized to steam also obviously declined and a remarkable decrease in P_M was expected. A similar phenomenon was found between Group C and Group D.

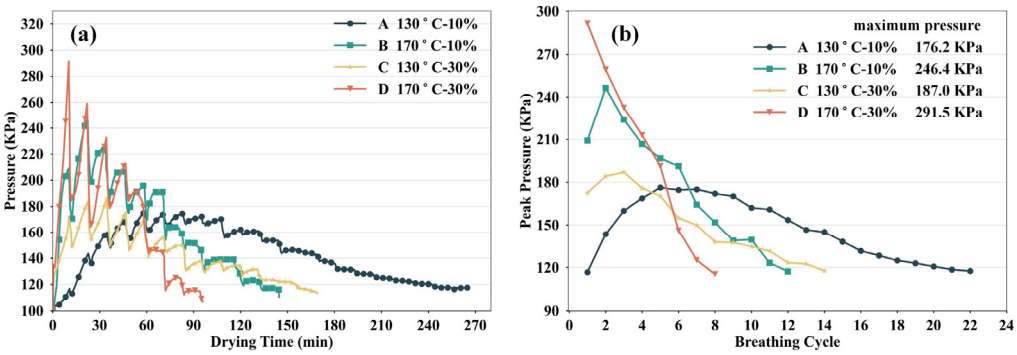

Figure 9. Internal pressure (**a**) and peak pressure (**b**) curves of dried lumber.

These results also indicated that the maximum P_M increased by 6.13% with the increase in R_c from 10% to 30% at 130 °C. And the corresponding increment was 18.30% at 170 °C. The reason was that thickness of lumber was decreased with increasing R_c, leading to a shortened heat transfer path and accelerated heat transfer. Therefore, a more complete vaporization of water inside the lumber was expected, resulting in a greater level of P_M. Furthermore, T_P showed a greater effect on maximum P_M than R_c. This may be related to the fact that the maximum T_M mainly depends on the T_P, which was analyzed in the previous section.

Figure 10 depicts the curves of the P_M drop value (the drop value in P_M after opening the heating plates) with a breathing cycle. The maximum P_M drop was increased with increasing T_P and R_c. An increment of 208.75% in the maximum P_M drop was observed with the increase in T_P from 130 to 170 °C at the R_c of 10%. The result was consistent with our previous studies [14] on poplar (*Populus tomentosa*) lumber. This could be explained via the increased maximum P_M of lumber at 170 °C. The migration of steam and water from the inner wood to the wood's surface was accelerated due to the greater pressure gradient between the lumber and the atmospheric environment in the opening period of heating platens [40], resulting in a higher maximum P_M drop. Furthermore, the extent of damage to the wood microstructure became severe with higher T_P (Figures 3–5), which may have led to improved gas permeability and accelerated pressure reduction.

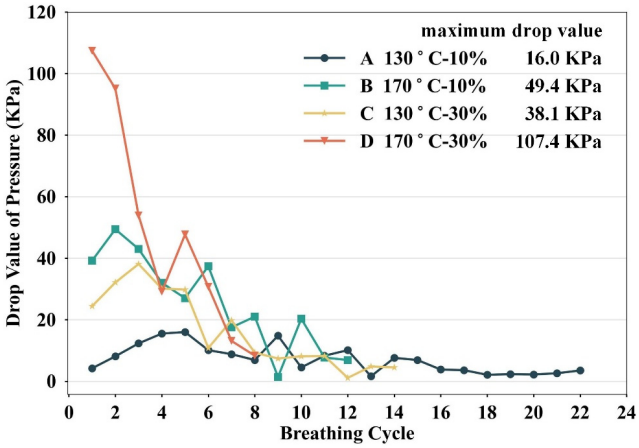

Figure 10. Pressure drop value curves of dried lumber.

It was also noted that the maximum P_M drop was increased by 138.13% when the R_c was increased from 10% to 30% at the T_P of 130 °C. This may be due to the fact that the extent of damage to the wood microstructure was increased and the steam migration path was shortened with increasing R_c, which made the steam move out more rapidly from inside lumber during the opening period of heating platens, thereby accelerating the reduction in P_M.

Overall, T_P and R_c are the two main operating parameters that affect the internal temperature and pressure variations in lumber during periodic hot-press drying. The influence of T_P on the internal temperature and pressure was greater than that of R_c. These results are basically consistent with the microstructural changes of dried lumber. Moreover, the fluctuating pressure was the main driving force, leading to moisture migration and mechanical damage of cell tissues in lumber. New pathways for fluid flow were formed due to the changes in wood microstructure and cell wall pore structure, and the permeability of lumber was increased, resulting in a further enhancement in the migration efficiency of moisture. Therefore, the drying rate was effectively increased with the increase in T_P and R_c during periodic hot-press drying.

4. Conclusions

Synergistic effects of heating platens' temperature and compression ratio on periodic the hot-press drying of Chinese fir lumber with a 30 mm thickness were investigated. The drying rate increased remarkably alongside increasing T_P and R_c. Damages were observed to the wood microstructure to various degrees after drying, and the damage became more severe with higher T_P and R_c. Detachments between ray parenchyma cells and longitudinal tracheids occurred at a T_P of 170 °C, which may have formed macro-cracks at a higher T_P and reduced drying quality. The number of pores in the pore diameter range of 2.5~6.2 nm was significantly increased with increasing T_P, resulting in the enlarged specific surface area and pore volume of the cell wall.

Internal temperature and pressure variations of lumber during the drying process were analyzed. The maximum T_M and P_M mainly depend on the T_P. The maximum T_M increased from 126.2 to 165.2 °C and the maximum P_M increased from 176.2 to 246.4 Kpa with the increase in T_P from 130 to 170 °C at the R_c of 10%. A similar result was found at the R_c of 30%. The fluctuating pressure was the main driving force of moisture migration and mechanical damage of cell tissues in lumber. Furthermore, the damage could generate new pathways for moisture migration and resulted in improved permeability, so the moisture was easier to move out from inside the lumber. The increased T_P and R_c contributed to accelerated moisture migration and decreased drying time. However, T_P should not be too high to prevent the pressure from causing severe damage to the wood's microstructure and significantly affect its mechanical properties.

Author Contributions: Conceptualization, J.H. and X.W.; methodology, J.H. and S.W.; validation, X.W. and X.Z.; formal analysis, X.W. and S.W.; resources, C.H.; data curation, S.W. and X.Z.; writing—original draft preparation, X.W. and J.H.; writing—review and editing, X.W., X.Z. and C.H.; visualization, X.W. and S.W.; supervision, J.H. and C.H.; project administration, J.H.; funding acquisition, J.H. and X.W. All authors have read and agreed to the published version of the manuscript.

Funding: This research was funded by the National Natural Science Foundation of China, grant number 32201492, 31670561; Talent Startup Project of Scientific Research and Development Foundation of Zhejiang A & F University, grant number 2021LFR042, 2020FR020.

Data Availability Statement: The data presented in this study are available on request from the corresponding authors.

Conflicts of Interest: The authors declare no conflicts of interest.

References

1. Guo, J.; Guo, X.; Xiao, F.; Xiong, C.; Yin, Y. Influences of provenance and rotation age on heartwood ratio, stem diameter and radial variation in tracheid dimension of cunninghamia lanceolata. *Eur. J. Wood Wood Prod.* **2018**, *76*, 669–677. [CrossRef]
2. Weng, X.; Zhou, Y.; Fu, Z.; Gao, X.; Zhou, F.; Jiang, J. Effects of microwave pretreatment on drying of 50 mm-thickness Chinese fir lumber. *J. Wood Sci.* **2021**, *67*, 13. [CrossRef]
3. He, S.; Lin, L.; Fu, F.; Zhou, Y.; Fan, M. Microwave Treatment for Enhancing the Liquid Permeability of Chinese Fir. *BioResources* **2014**, *9*, 1924–1938. [CrossRef]
4. Tang, Y.F.; Hart, C.A.; Simpson, W.T. A numerical model for heat transfer and moisture evaporation processes in hot-press drying: An integral approach. *Wood Fiber. Sci.* **1994**, *26*, 78–90.
5. Zhuang, S.Z. Some comments on the technological innovation and development of wood drying in China. *China For. Prod. Ind.* **2008**, *35*, 6–9. (In Chinese)
6. Wang, M.; Zhang, M.; Lu, Z.; Jia, W. Hot pressing technology investigation of light-weight wooden brick. *Constr. Build. Mater.* **2020**, *265*, 120426. [CrossRef]
7. Bond, B.H.; Espinoza, O. A decade of Improved Lumber Drying Technology. *Curr. Forest. Rep.* **2016**, *2*, 106–118. [CrossRef]
8. Han, C.; Xu, J.; Jiang, J.L.; Jiang, J.H.; Lv, J. Moisture content distribution of multiple *eucalyptus* veneers during hot-press-drying. *Wood Res.* **2014**, *59*, 351–358.
9. Unsal, O.; Candan, Z. Moisture content, vertical density profile and Janka hardness of thermally compressed pine wood panels as a function of press pressure and temperature. *Dry. Technol.* **2008**, *26*, 1165–1169. [CrossRef]
10. Simpson, W.T.; Pearson, R.G.; Tang, Y.F. Press-drying plantation loblolly pine lumber to reduce warp: Follow-up studies. *For. Prod. J.* **1992**, *42*, 65–69.
11. Unsal, O.; Candan, Z.; Korkut, S. Wettability and roughness characteristics of modified wood boards using a hot-press. *Ind. Crops Prod.* **2011**, *34*, 1455–1457. [CrossRef]
12. Li, X.; Zhang, B.; Li, W. Microwave-Vacuum drying of wood: Model formulation and verification. *Dry. Technol.* **2008**, *26*, 1382–1387. [CrossRef]
13. Ramon, G.; Agnon, Y.; Dosoretz, C. Heat transfer in vacuum membrane distillation: Effect of velocity slip. *J. Membr. Sci.* **2009**, *331*, 117–125. [CrossRef]
14. Hou, J.; Yi, S.; Zhou, Y.; Pan, B. Moisture state variety in poplar lumber with moisture content above fibre saturation point during hot-press drying. *J. Wood Sci.* **2018**, *64*, 730–737. [CrossRef]
15. Nguyen, D.V.; Nguyen, T.T.H.; Kubota, S.; Suzuki, S. Effects of size and type of raw material on temperature and vapour pressure behaviour of wood-based panels during hot-pressing. *Wood Mater. Sci. Eng.* **2021**, *17*, 702–711. [CrossRef]
16. Zhou, Y.; Fu, F.; Li, X.; Jiang, X.; Chen, Z. Effects of microwave treatment on residue growth stress and microstructure of Eucalyptus urophylla. *J. Beijing For. Univ.* **2009**, *31*, 146–150. (In Chinese)
17. Hou, J. Periodic Hot-Platen Drying and Heat & Mass Transfer Mechanism of Poplar Lumber. Ph.D. Thesis, Beijing Forestry University, Beijing, China, 2019.
18. Torgovnikov, G.; Vinden, P. High-Intensity microwave wood modification for increasing permeability. *For. Prod. J.* **2009**, *59*, 84–92.
19. Torgovnikov, G.; Vinden, P. Microwave wood modification technology and its applications. *For. Prod. J.* **2010**, *60*, 173–182. [CrossRef]
20. Wang, Y.; Gu, L.; Liu, Q.; Du, G. Mathematical models of moisture transfer in press drying of Pinus massoniana lumber. *J. Nanjing For. Univ.* **2005**, *32*, 71–75. (In Chinese)
21. Wang, Y.; Gu, L.; Wang, C.; Ke, S. Regularity of heat transfer during press drying of Pinus massoniana lumber. *J. Nanjing For. Univ.* **2008**, *29*, 33–36. (In Chinese)
22. Dogu, D.; Tirak, K.; Candan, Z.; Unsal, O. Anatomical investigation of thermally compressed wood panels. *BioResources* **2010**, *5*, 2640–2663. [CrossRef]
23. Schrepfer, V.; Schweingruber, F.H. Anatomical structure in reshaped press-dried wood. *Holzforschung* **1998**, *52*, 615–622. [CrossRef]

24. Chen, H.Y.; Lang, Q.; Zhang, H.; Wu, G.F.; Zheng, X.; Pu, J.W. Study of chemical modification by impregnation of fresh Poplar Log and hot-pressed drying process. *BioResources* **2013**, *8*, 3924–3933. [CrossRef]
25. Huang, R.; Feng, S.; Gao, Z.Q. Effect of water/moisture migration in wood preheated by hot press on sandwich compression formation. *Holzforschung* **2022**, *76*, 11–12. [CrossRef]
26. *GB/T 6491-2012*; Drying Quality of Sawn Timber. Standardization Administration of the People's Republic of China: Beijing, China, 2012.
27. Zhou, F.; Gao, X.; Fu, Z.; Zhou, Y. Drying kinetics of poplar lumber during periodic hot-press drying. *Dry. Technol.* **2018**, *36*, 1767–1780. [CrossRef]
28. Zhang, Y.; Jia, K.; Cai, L.; Shi, S.Q. Acceleration of moisture migration in larch wood through microwave pre-treatments. *Dry. Technol.* **2013**, *31*, 666–671. [CrossRef]
29. He, X.; Xiong, X.; Xie, J.; Li, Y.; Wei, Y.; Quan, P.; Mou, Q.; Li, X. Effect of microwave pretreatment on permeability and drying properties of wood. *BioResources* **2017**, *12*, 3850–3863. [CrossRef]
30. Erickson, H.D. Permeability of southern pine wood-a review. *Wood Sci.* **1970**, *2*, 149–158.
31. Tong, Y.; Zhao, G. Structure of Bordered Pit Membrane of Cunninghamia lanceolata Tracheid. *Sci. Silvae Sin.* **2007**, *43*, 151–153. (In Chinese)
32. Zhang, Y.; Cai, L. Effects of steam explosion on wood appearance and structure of sub-alpine fir. *Wood Sci. Technol.* **2006**, *40*, 427–436. [CrossRef]
33. Balboni, B.M.; Ozarska, B.; Garcia, J.N.; Torgovnikov, G. Microwave treatment of eucalyptus macrorhyncha timber for reducing drying defects and its impact on physical and mechanical wood properties. *Eur. J. Wood Wood Prod.* **2018**, *76*, 861–870. [CrossRef]
34. Xia, J.; Zhang, Y.; Cai, J. Opening cell pathways of larch wood by steam explosion. *J. Fujian Agric. For. Univ.* **2013**, *42*, 543–547. (In Chinese)
35. Muzamal, M.; Gamstedt, E.K.; Rasmuson, A. Mechanistic study of microstructural deformation and stress in steam-exploded softwood. *Wood Sci. Technol.* **2017**, *51*, 447–462. [CrossRef]
36. Lu, J.; Bao, F. Effect of steaming on the permeability of wood. *Sci. Silvae Sin.* **1994**, *30*, 352–357. (In Chinese)
37. Yin, J. Effect of Compression Combined with Steam Treatment on the Structure and Properties of Cell Walls of *Cunninghamia lanceolata*. Ph.D. Thesis, Chinese Academy of Forestry, Beijing, China, 2016.
38. García, P.J.; Avramidis, S.; Lam, F. Internal temperature and pressure responses to flake alignment during hot-press drying. *Holz Roh Werkst.* **2001**, *9*, 425–431.
39. Rofi, M.N.; Kubota, S.; Kobori, H.; Kojima, Y.; Suzuki, S. Furnish type and mat density effects on temperature and steam pressure of wood-based panel during hot pressing. *J. Wood Sci.* **2016**, *62*, 168–173. [CrossRef]
40. Rofi, M.N.; Yamamoto, N.; Kojima, Y.; Suzuki, S. Effect of furnish on temperature and vapor pressure behavior in the center of mat panels during hot pressing. *J. Math. Fund. Sci.* **2014**, *46*, 175–182. [CrossRef]